MATEC Web of Conferences **33**, 03006 (2015)
DOI: 10.1051/matecconf/20153303006

Adhesion at TiNi interfaces with Ta, Mo and Si

Alexander Bakulin[1,2], Konstantin Tarasov[2], Lyudmila Meisner[1] and Svetlana Kulkova[1,2a]

[1]*Institute of Strength Physics and Materials Science of Siberian Branch Russian Academy of Sciences, pr. Akademichesky 2/4, Tomsk 634055, Russia*
[2]*National Research Tomsk State University, pr. Lenina 36, Tomsk 634050, Russia*

Abstract. Atomic and electronic structure of (001) and (110) interfaces between TiNi and Ta, Mo, Si thin films are investigated by *ab-initio* method within density functional theory. It is shown that high adhesion properties can be attained at the Mo/TiNi(001)$_{Ti}$ interface, whereas the work of separation of Ta and Si films from alloy is substantial less. We found that the work of separation in case of (110) interface is lower than that at (001). Structural and electronic properties of considered interfaces are analysed. Our calculations of metal-oxide interfaces demonstrate that formation of intermediate titanium oxides layers can result in decrease of adhesion at Me/TiNi(110) interfaces.

1 Introduction

Intermetallic TiNi alloy exhibiting excellent mechanical properties such as the shape memory effect, superelasticity, reversible strain recovery without materials failure, etc. has widespread application in industry and medicine. In the latter case TiNi and TiNi-based alloys are used for manufacturing different implants and fixation devices. It is known that the interaction between implant material and human tissue is fundamental issue of medicine. Materials used for medical applications must provide a high biocompatibility [1]. Physicochemical and biological aspects of TiNi were considered in [2-4]. The biocompatibility of TiNi is due to formation of inert titanium dioxide layers which effectively passivate alloy surface. To prevent the release of Ni and improve the biocompatibility and corrosion resistance of implants it is necessary to modify their surface properties only because surface or thin surface layers are in contact with blood and body tissue. For this goal appropriate surface treatment by ion beams or deposition of thin coatings of biotolerable chemical elements are applied [5,6]. As was shown in literature elements such as Zr, Ta, Si are very promising for this purpose [7-10]. However, the influence of metal and silicon coatings on the corrosion resistance is not completely understood [10]. In relevant literature [11-13] it was shown experimentally and theoretically that the presence of a thin layer of potassium on the TiNi surface enhances the oxidation of surface Ti atoms. It is known that alkali metals (K and Na) in small amounts are harmless for the body. The influence of the Si-doping on the corrosion resistance of Ti-based alloys was demonstrated experimentally in [9,10]. It is believed that the formation titanium-based metal-ceramic composite consisting of oxide, silicides, etc. in surface layers is the main reason of corrosion resistance improvement after ion-beam treatment. We would like to remind also that the formation of oxide layers on pure TiNi surface was considered by theoretical approaches in [14-17]. Alloy-oxide interface was studied in details experimentally in [18]. However the adhesion properties of different coatings have not been studied by theoretical approaches.

It is known that the work of separation (W_{sep}) is a fundamental quantity, which controls the mechanical strength of the metal-alloy interfaces. It is the reversible work needed for separation of interface into two free surfaces. The first principles methods are good tool to study this property.

The aim of this work is to study the atomic and electronic structure and also adhesion properties of interfaces between TiNi and Ta, Mo, Si thin films in dependence of their orientation and termination of the alloy surface.

2 Computational details

Atomic structures and electronic properties of (001) and (110) interfaces between TiNi and Ta, Mo, Si were investigated using pseudopotential approach implemented in the Vienna *ab initio* simulation package (VASP) [19,20]. The generalized gradient approximation [21] for the exchange-correlation functional was applied. The plane wave basis was used to describe the valence electronic states. The energy cutoff for plane waves was set as 500 eV. We adopted the Monkhorst-Pack *k*-points mesh (15×15×15) for bulk TiNi, Ta, Mo, Si and (9×9×15) for TiO_2. The *k*-points mesh (7×7×1) was applied for surface and interface calculations. The total energies were converged up to 10^{-4} eV. With these setups, we got equilibrium lattice parameter of a = 3.011 Å for

[a] Corresponding author: kulkova@ms.tsc.ru

bulk TiNi, 3.292 Å for Ta, 3.155 Å for Mo, 5.455 Å for Si and a = 4.611 Å, c = 2.959 Å for the rutile TiO_2, all in good agreement with experimental measurements [22].

In order to describe Me/TiNi(001) and Me/TiNi(110) interfaces a symmetrical slabs model with seven layers of alloy and four-six layers of metals on both sides of alloy surfaces was used. The vacuum thickness between slabs was of ~10 Å. The three central layers were fixed at the bulk position but other atoms were relaxed until the forces acting on the atoms are less than 0.01 eV/Å. In the case of Si/TiNi interfaces the surface cell of TiNi(2×2) was used in order to coincide with Si thin film.

For the description of Me/TiO_2(100) interface eight metal layers on one side of oxide surface and 17-19 atomic layers of oxide in dependence on its surface terminatio were used. More information about this interface will be given later.

The work of separation (W_{sep}) is defined as

$$W_{sep} = (E_{Me} + E_{\mathrm{TiNi}} - E_{Me/\mathrm{TiNi}})/2S \qquad (1)$$

where $E_{\mathrm{Me/TiNi}}$ is the total energy of supercell containing the multilayered slabs, E_{Me} and E_{TiNi} are the total energies of the same supercell containing a single slab of the metal or alloy (oxide), respectively. Note that S in (1) is the interface area and the factor 2 takes into account the presence of the two equivalent interfaces within a computational cell.

3 Results and discussion

3.1 Atomic and electronic structure of Me/TiNi(001) and Me/TiNi(110) interfaces

Atomic structure of the Me/TiNi(001) interface is given in Fig. 1a. It is necessary to point out that TiNi alloy along [001] direction represents alternating atomic layers of Ti and Ni that leads to two surface terminations: Ni- and Ti-terminated surface. The H-hollow configuration of metal film with interfacial metal atom which continues the alloy structure was found to be preferential on both TiNi(001) surface terminations.

The calculated values of the work of separation are given in table 1. It is seen that for both Ta and Mo films high values of W_{sep} are calculated for $Me/TiNi(001)_{Ti}$ interface with Ti interfacial layer. Higher value of the work of separation (6.13 J/m^2) for the interface (001) with Mo film correlates with smaller value of the interfacial distance (1.65 Å). The similar trend is obtained for $Me/TiNi(001)_{Ni}$ with Ni interfacial layer. It should be noted that the growth of Mo film on TiNi surface causes less strain in the interfacial layers due to small mismatch between Mo and TiNi lattices (4.47%).

Atomic structure of Me/TiNi(110) interface is given in Fig.1b. Since TiNi(110) surface is stoichiometric one both Ti and Ni atoms locate in the interfacial layer. One can see from Table 1 that the chemical bond at the (110) interface with Mo is only slightly stronger than that with Ta.

As in previous case the higher value of the work of separation at Mo/TiNi(110) correlates with smaller

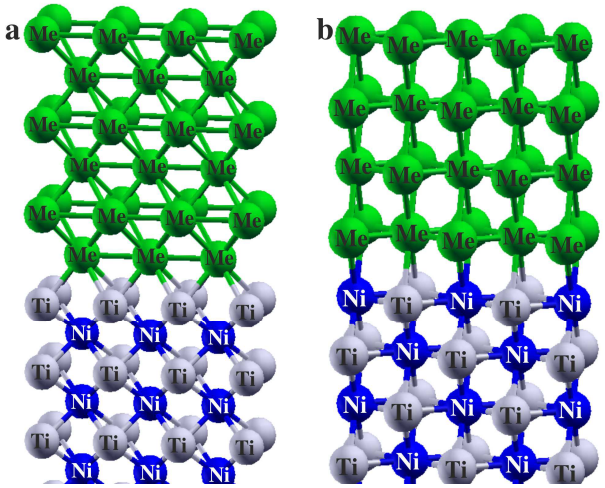

Figure 1. Atomic structure of Me/TiNi(001) (a) and Me/TiNi(110) (b) interfaces. Upper part of the structure is given only on this figure.

interfacial distance. It is seen from Fig. 1 that in this case the metal atom has two bonds with alloy surface atoms whereas it is fourfold coordinated in the most stable H hollow configuration at the (001) interface. At the same time the interatomic distances between nearest interfacial atoms at the (110) interface change insignificantly: the Mo-Ti distance increases by 0.07 Å but Mo-Ni distance decreases by 0.08 Å. The distances between other interfacial atoms are larger than the sum of their atomic radii (2.99-3.19Å). They contribute in the chemical bond indirectly through the hybridisation with alloy nearest atoms at the surface layer. The number of bonds on the contact area is smaller in the case of the Me/TiNi(110) interface. All these factors provide the decrease of W_{sep} at the (110) interface. In general, decrease of W_{sep} at the (110) interface in comparison with (001) one agrees well with increase of interlayer distance in alloy and metals in this direction, and, as consequence, with increase of interfacial distance (Table 1) as well.

Let's to discuss the electronic structure of Me/TiNi(001) interface. Local densities of states (DOS) of interfacial atoms are given in Fig. 2. The presence of an additional electron in Mo d-band leads to its shift below the Fermi energy (E_F) in comparison with Ta d-band. This reflects on the hybridisation of Mo atom orbitals with s,d-states of Ti interfacial atom which is stronger than that in case of Ta. This conclusion is also confirmed by the total charge density distribution (Fig. 3). It is seen that concentration of isolines at Mo-Ti bond is greater than that at Ta-Ti one. In general, the distribution of charge density at this interface

Table 1. Work of separation and interfacial distance (d) at Me/TiNi(001) and Me/TiNi(110) interfaces.

Interface (001)	$Ta/TiNi_{Ti}$	$Ta/TiNi_{Ni}$	$Mo/TiNi_{Ti}$	$Mo/TiNi_{Ni}$
W_{sep}, J/m^2	4.89	4.55	6.13	4.27
d, Å	1.84	1.61	1.65	1.68
Interface (110)	Ta/TiNi		Mo/TiNi	
W_{sep}, J/m^2	4.04		4.31	
d, Å	2.19-2.48		2.10-2.38	

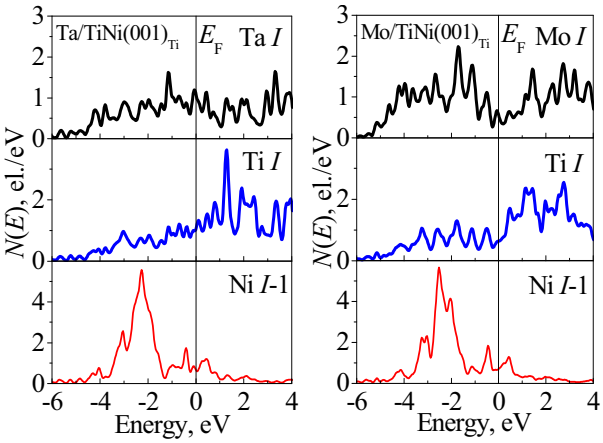

Figure 2. Local densities of states of atoms at the Me/TiNi(001) interface. Symbols I and I-1denote interface and subinterface layers.

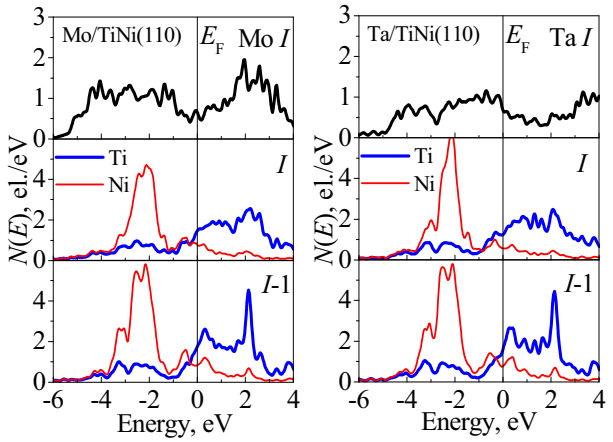

Figure 4. Local densities of states of atoms at the Me/TiNi(110) interface. Symbols I and I-1denote interface and sub-interface layers.

demonstrates typical for metallic bonding behaviour. Alongside with bonding between interfacial atoms of BCC metals and Ti it is seen the increase of bonding within two atomic layers in the metal film as well. This effect is more pronounced for Mo thin film.

Peaks of Ti occupied band (Fig. 2) coincide well with those of Mo that indicates also on their strong interaction. On other hand Ni *d*-band is almost fully occupied that leads to appearance of sharp peak just below E_F as one can see in Fig. 2 for Ni sub-interfacial atom. Since the states of Ni are localized in narrow energy region it is difficult for them to be involved in the interaction with Mo or Ta interfacial atoms. Besides the presence of an additional electron in the Mo *d*-band can provide the repulsion between Mo and Ni orbitals due to the Pauli principle. In spite of smaller interfacial distance at the interface of metals with the Ni-terminated TiNi(001) surface due to size effect (smaller radius of Ni atom than that of Ti one), electronic factors mentioned above are responsible for decrease of the adhesion at the Me/TiNi(001)$_{Ni}$ interface.

Finally the local densities of interfacial atoms at the Me/TiNi(110) interface are presented in Fig. 4. In this case the interpretation of DOS curves is much easier because their structure for alloy atoms is almost similar and only small difference in valence bands of Ta and Mo can be seen. As was mentioned above the hybridization of Mo with Ti orbitals is slightly stronger than that between Ta and Ti states however the opposite effect takes place in case of interaction of Mo or Ta with Ni. The competition of these factors leads to small difference in W_{sep}.

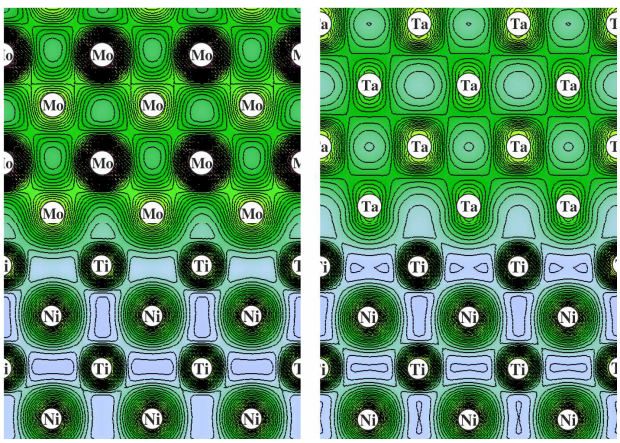

Figure 3. Total charge density distribution at Mo/TiNi(001)$_{Ti}$ (left) and Ta/TiNi(001)$_{Ti}$ (right) interfaces in the plane which crosses the Me-Ti bonds.

3.2 Atomic and electronic structure of Si/TiNi(001) and Si/TiNi(110) interfaces

Atomic structure of the Si/TiNi(001) interface are given in Fig. 5. In this case TiNi(2×2) surface cell was used to match better silicon one. We remind that Si has diamond-like structure. Three configurations (H, B, T) of Si film shown in Fig. 5 were considered on both terminations of TiNi(001) surface. As follows from our calculations, the interface with *H*-configuration of Si film is most preferential (Table 2). It is seen that the difference in the work of separation of silicon film from both TiNi(001) surface terminations is enough small ~0.1-0.2 J/m^2. The values of W_{sep} for the *B* or *T* configurations are substantial less in comparison with *H*-configuration. In general, the chemical bonding at the (001) interface with Si is weaker than that at the interface

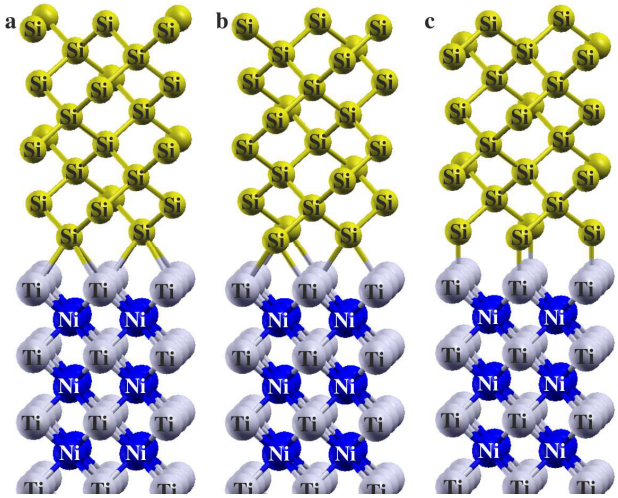

Figure 5. Atomic structure of Si/TiNi(001) interface in dependence on the configuration of Si film: a) *H*-hollow configuration; b) *B*-bridge configuration; c) *T*-top configuration.

Table 2. Work of separation and interface distance (d) at Si/TiNi(001) and (110) interfaces.

Interface	$Si(001)/TiNi(001)_{Ti}$			$Si(001)/TiNi(001)_{Ni}$		
Configuration	*H*	*B*	*T*	*H*	*B*	*T*
W_{sep} (J/m^2)	3.67	2.81	2.32	3.57	2.66	2.12
d (Å)	1.55	2.05	2.20	1.15	1.67	2.10

with transition metals. This can be understood from atomic and electronic structure of such interfaces. First of all it is necessary to take into account that Si has *s*- and *p*-states only. The hybridization of *s*,*p*-states with *s*,*d*-orbitals of Ti or Ni is much weaker than hybridization between interfacial atoms of transition metals.

In spite of *s*-states of Si locate below bottom of Ti or Ni valence bands one can see in Fig. 6 small peaks on their s partial DOS curves which are induced by interaction with Si film. Silicon *p*-states contribute more in Si-Ti(Ni) interaction because they locate in the same energy region as occupied part of Ti (Ni) valence bands.

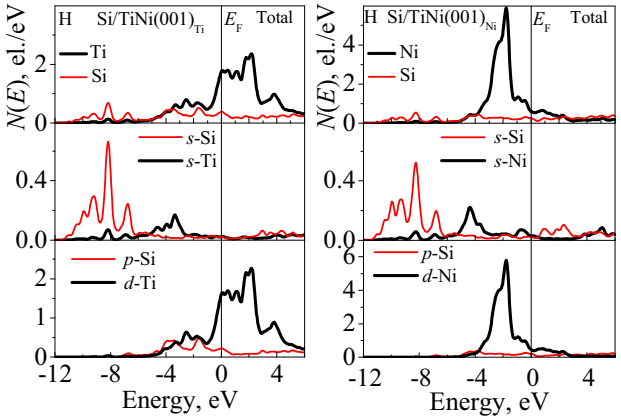

Figure 6. Partial densities of states of atoms at the Si/TiNi(001) interface.

The correlation between W_{sep} and interfacial distance is also valid in set of the considered Si film configurations. It should be noted that the interfacial distances at Ni-terminated interface are smaller than those at Ti-terminated one due to the size effect mentioned above. Smaller number of bonds formed at Si/TiNi interfaces than those at Me/TiNi is also responsible for decrease of the adhesion properties of Si film (Fig. 7). Charge density distributions confirm weaker bonding at Si/TiNi interfaces. It is seen in Fig. 7 covalent bonding within Si film and metal-covalent bonding between interfacial atoms for both (001) and (110) interfaces.

Note that at the $Si/TiNi(001)_{Ti}$ interface the extension of first interlayer distance (~8.13%) in alloy was calculated whereas at $Si/TiNi(001)_{Ni}$ the compresion of this distance of 5.14% takes place. In case of clean TiNi(001) surface, the large inward relaxation of the first interlayer distance was obtained for both alloy surface terminations [23,24]. The smaller change of this distance at $Si/TiNi(001)_{Ni}$ interface can be also explained by weaker chemical reactivity of Ni interfacial atoms. The chemical reactivity of Ti interfacial atoms leads to restore of first interlayer distance up to bulk value and moreover

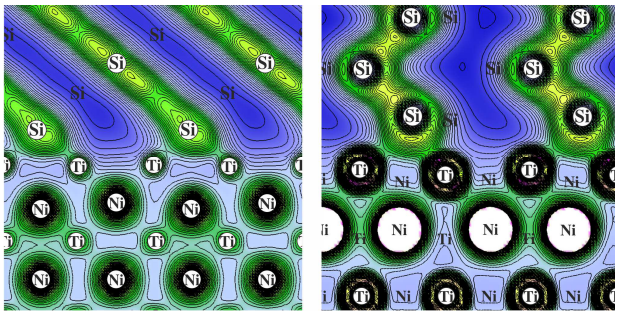

Figure 7. Total charge density distribution at $Si/TiNi(001)_{Ti}$ (left) and Si/TiNi(110) (right) interfaces in the plane which crosses the Si-Ti bonds in the case of (001) interface and in the plane which crosses Si and Ti interfacial atoms in case of (110) interface.

to its following extension. The similar trend is valid for all considered configurations of Si film.

Several words should be said about Si/TiNi(110) interface. As in previous case of Me/TiNi(110) interface the work of separation of Si film from TiNi(110) surface is significant lower (2.18 J/m^2) than that for Si/TiNi(001). The decrease of W_{sep} at this interface is connected with the same reason as for metal-alloy interface: the increase of interfacial distance leads to weaker hybridization of Si *s*,*p*-orbitals with *s*,*d*-states of both Ti and Ni interfacial atoms.

Finally, it should be noted that the lattice parameter of Si is compressed of ~10% in respect to alloy one that causes large strain at the both (001) and (110) interfaces. On other hand the extention of lattice in the interfacial plane leads to compresion of interlayer distance in perpendicular direction to interface. This increases adhesion properies of Si coatings. Easier oxidation of silicon surface provide also good biocompantibility of this material. As was shown in the literature [9] Si-doping of Ti-based alloys can improve their corrosion resistance.

3.3 Atomic and electronic structure of Me(110)/TiO_2(100) interface

Intermediate oxide layers existing at the metal-alloy interface may have influence on adhesion properties. In this connection we investigated the properties of metal-oxide interfaces also. In order to determine the most stable surface termination of alloy or oxide, the surface energy (σ) as function of chemical potential of Ti should be calculated.

The surface energy can be calculated using the following equation

$$\sigma = \frac{1}{2S}\left[E_{tot}^{slab} - N_{Ti}\mu_{Ti} - N_{Ni}\mu_{Ni}\right] \qquad (2)$$

where E_{tot}^{slab} is total energy of a slab that contains N_{Ti} and N_{Ni} atoms of Ti and Ni, respectively. Here μ_{Ti} and μ_{Ni} are chemical potentials of Ti and Ni. S is the surface area.

For the stoichiometric surface, we may take directly the bulk energy of alloy as reference as shown by Eq. (3)

$$\sigma = \frac{1}{2S}(E_{tot}^{slab} - N\mu_{TiNi}^{bulk}). \quad (3)$$

However, for the non-stoichiometric surface, Eq. (3) is not applicable any more. The surface energy should be defined as:

$$\sigma = \frac{1}{2S}\left[E_{tot}^{slab} - N_{Ni}\mu_{TiNi} - \mu_{Ti}(N_{Ti} - N_{Ni})\right]. \quad (4)$$

It is necessary to note that μ_{Ti} is restricted by upper limits $\mu_{Ti} \le \mu_{Ti}^{bulk}$. So, the equation (4) can be represented as function of the relative chemical potential of Ti with respect to its bulk phase

$$\sigma = \frac{1}{2S}[E_{tot}^{slab} - N_{Ni}\mu_{TiNi}^{bulk} - \mu_{Ti}^{bulk}(N_{Ti} - N_{Ni}) - \Delta\mu_{Ti}(N_{Ti} - N_{Ni})], \quad (5)$$

where $\Delta\mu_{Ti} = \mu_{Ti} - \mu_{Ti}^{bulk}$ varies in the range of $-\Delta H \le \Delta\mu_{Ti} \le 0$ and ΔH (0.739 eV) is the heat of formation of TiNi alloy. More details are given in [25]. Our calculations show that TiNi(110) surface is stable up to $\Delta\mu_{Ti}$ > -0.46 eV. In the Ni-rich limit the Ni-terminated (001) surface is found to be stable.

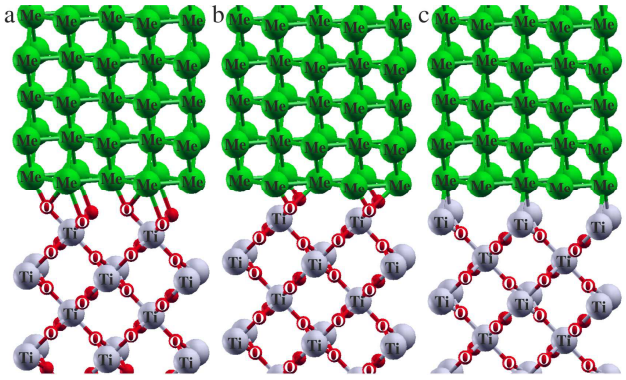

Figure 8. Atomic structure of Me/TiO_2(100) interface in dependence on interfacial oxide layers: a) two oxygen layers; b) one oxygen layer; c) Ti layer.

We remind that the TiO_2(100)/TiNi(110) interface was considered in our previous investigations [14,17] due to good lattice matching of the alloy and oxide surfaces. The atomic structure of Me(110)/TiO_2(100) interface is given in Fig. 8. It is seen that TiO_2(100) has three possible surface terminations. The calculations of surface energy (Fig. 9) using similar equations which was described above demonstrate that $TiO_2(100)_O$ surface terminated by one atomic layer of oxygen is stable among three considered terminations.

The calculated work of separation of metal films from oxide surface are given in Table 3. It is seen that higher values of W_{sep} correspond unstable interface Me/$TiO_2(100)_{2O}$ with two interfacial oxygen layers. The work of separation at stable Me/$TiO_2(100)_O$ interface is substantional lower. An increase of adhesion of Mo film at Mo/$TiO_2(100)_{Ti}$ interface with Ti-terminated oxide surface in comparison with Ta film corresponds to trend obtained at metal-alloy interfaces.

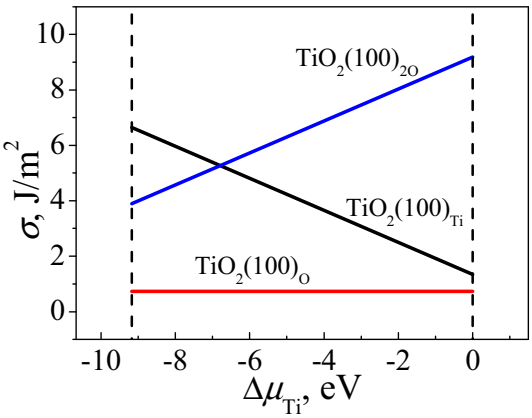

Figure 9. Surface energies of different TiO_2(100) surface terminations versus titanium chemical potential.

Table 3. Work of separation and interface distance (d) at Me/TiO_2(100) interface.

Interface	Ta(110)/ $TiO_2(100)_{2O}$	Ta(110)/ $TiO_2(100)_O$	Ta(110)/ $TiO_2(100)_{Ti}$
W_{sep} (J/m²)	10.33	2.34	1.73
d (Å)	1.35	1.48	2.62
Interface	Mo(110)/ $TiO_2(100)_{2O}$	Mo(110)/ $TiO_2(100)_O$	Mo(110)/ $TiO_2(100)_{Ti}$/
W_{sep} (J/m²)	8.47	1.66	1.97
d (Å)	1.30	1.45	2.44

It is seen in Fig. 10 that the interaction of Ta atom with oxygen interfacial atom is stronger than that of Mo. Both s- and p-valence bands of O interfacial atom are shifted deeper of 0.2-0.5 eV at the Ta/$TiO_2(100)_O$ interface in comparison with Mo/$TiO_2(100)_O$. The states of next from interface Ti layer are also involved in the interaction with s-states of oxygen. Small peaks on the Ti DOS curve induced by interaction with O states can be seen around -20 eV. The center of gravity of p-valence band of O sub-interfacial atom is also shifted more pronounced in case of Ta that indicates its indirect interaction with metal film.

We would like to emphasize that the structure of TiO_2(100) surface represents the alternation of Ti layer and two oxygen layers. It is known that two O atoms in material prefer to be far from each other. In this connection cleavage between two oxygen layers needs

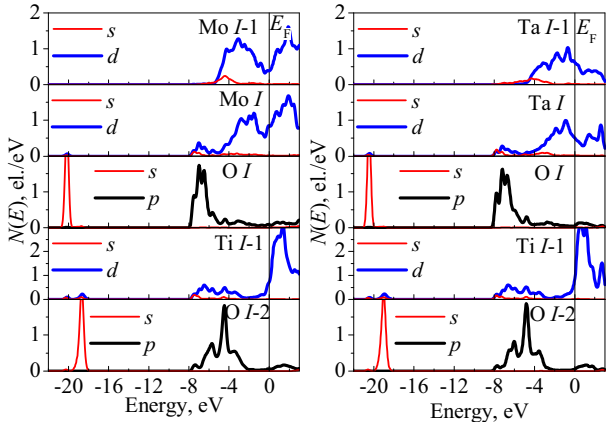

Figure 10. Local DOS at Me(110)/$TiO_2(100)_O$ interface with Mo (left) and Ta (right).

less energy. Our simulation of such cleavage between Mo film with oxygen layer and $TiO_2(100)_O$ shows that W_{sep} decreases significantly up to 1.23 J/m^2. The calculations of work of the separation in dependence on cleavage plane allow us to conclude that the cleavage between two O layers is more preferable than that between metal and oxygen terminated $TiO_2(100)$ film. Similar results were obtained at $TiNi(110)/TiO_2(100)$ interface. Thus, the formation of intermediate oxide layers at the Me/TiNi interface has negative impact on adhesion properties of the metal films.

4 Summary

First principles method within density functional theory was applied to estimate the adhesion properties of Ta, Mo and Si films on oriented TiNi surfaces. Our results demonstrate that the work of separation of Mo thin films is greater than that of Ta or Si irrespective of the interface orientation. It was established that for different configurations of metal film on both alloy and oxide surfaces a higher adhesion corresponds to the configuration with smaller interfacial distance. Analysis of electronic structure of interfaces show that hybridisation of *s*,*d*-states of transition metals with TiNi alloy valence band is stronger than that of *s*,*p*-states of Si. The filling of *d*-band of Mo leads to its shift below the Fermi level that contributes to chemical bonding at interface and increase the adhesion properties of Mo thin film in comparison with Ta one. Formation of intermediate oxide layers at Me/TiNi interfaces leads to decrease of adhesion properties. The obtained results are in qualitative agreement with the experimental ones which will be discussed in our forthcoming paper.

Acknowledgement

The authors acknowledge the financial support from RFBR (research project N 14-02-91150_a_NSFC) and NSFC (project N 513111054) for the Chinese–Russian Co-operation. The work was partially supported by the Tomsk State University Competitiveness Improvement Program. Computations were performed using the SKIF-Cyberia supercomputer of National Research Tomsk State University.

References

1. G. Mani, M.D. Feldman, D. Patel, C.M. Agrawal, Biomaterials, **28**, 1689 (2007)
2. V.E. Gunter, V.I. Itin, L.A. Monasevich, et al., *Shape memory effects and their application in medicine* (Nauka, Novosibirsk, 1992)
3. S.A. Shabalovskaya, Int. Mater. Rev., **46**, 1 (2001)
4. S.A. Shabalovskaya, Acta Biomaterialia **4**, 447 (2008)
5. L.L. Meisner, Fiz. Mesomekh., **7**(S2) 169 (2004) [in Russian]
6. A.I. Lotkov, L.L. Meisner, V.N. Grishkov, Phys. Met. Metallogr., **99**(5), 508 (2005)
7. L.L. Meisner, A.I. Lotkov, V.A. Matveeva, L.V. Artemieva, S.N. Meisner, A.L. Matveev, Adv. Mater. Sci. Eng., **2012**, 706094 (2012)
8. L.L. Meisner, V.A. Matveeva, A.I. Lotkov, S.G. Psakhie, L.V. Artemieva, S.N. Meisner, A.L. Matveev, Izv. Vysshikh Uchebn. Zaved. Fizika, **54**, 39 (2011) [in Russian]
9. Z. Jiang, X. Dai, H. Middleton, Mater. Sci. Eng. B, **176**, 79 (2011)
10. S.G. Psakhie. S.N. Meisner, A.I. Lotkov, L.L. Meisner, A. V. Tverdokhlebova, J. Mater. Eng. Perform., **23**, 2620 (2014)
11. K.N. Nigussa, J.A. Stovneng, Phys. Rev. B, **82**, 245401 (2010)
12. K.N. Nigussa, J.A. Stovneng, Comput. Phys. Commun., **182**, 1979 (2011)
13. H. Tollefsen, S. Raaen, J. Appl. Phys., **105,** 123501 (2009)
14. S.E. Kulkova, V.E. Egorushkin, S.V. Eremeev, S.S. Kulkov, Mater. Sci. Eng. A, **438**, 476 (2006)
15. M. Nolan, S.A.M. Tofail, Biomaterials, **31**, 3439 (2010)
16. M. Nolan, S.A.M. Tofail, Phys. Chem. Chem. Phys., **12**, 9742 (2010)
17. S.E. Kulkova, A.V. Bakulin, Q.M. Hu, R. Yang, Physica B, **426**, 118 (2013).
18. H. Tian, D. Schryvers, D. Liu, Q. Jiang, J. Van Humbeeck, Acta Biomaterialia, **7**, 892 (2011)
19. G. Kresse, J. Furthmüller, Phys. Rev. B, **54**, 11169 (1996)
20. G. Kresse, J. Furthmüller, Comput. Mater. Sci., **6**, 15 (1996)
21. J.P. Perdew, J.A. Chevary, S.H. Vosko, K.A. Jackson, M.R. Pederson, D.J. Singh, C. Fiolhais, Phys. Rev. B, **46**, 6671 (1992)
22. C.I. Smithells, *Metals References Book* (Butterworth, London, 1976)
23. S.E. Kulkova, D.V. Valujsky, J.S. Kim, G. Lee, Y.M. Koo, Phys. Rev B, **65**, 085410 (2002)
24. S.A. Kulkov, S.V. Eremeev, S.E. Kulkova, Phys. Solid State, **51**, 1281 (2009)
25. L. Wang, J.X. Shang, F.H. Wang, Y. Zhang, A. Chroneos, J. Phys.: Condens. Matter, **23**, 265009 (2011)